Reconstruction Image Quality Theory
Evaluation of Filtered Back-Projection and Ordered-Subset Expectation Maximization

Herfried Wieczorek

Philips Research Laboratories, Aachen, Germany
`herfried.wieczorek@philips.com`

Abstract. We have developed an image quality theory for reconstruction that we apply to filtered back-projection (FBP) and statistical reconstruction (OSEM) for Single Photon Emission Computed Tomography (SPECT). Quantitative measures of reconstruction performance are given in terms of signal and noise power spectra, SPS and NPS, that we derive from phantom images. This allows evaluating the properties of statistical reconstruction, especially signal recovery, noise, impact of phantom size, and detector resolution. Our analysis shows how noise in reconstructed images is reduced by iterative resolution recovery.

1   Introduction

Single Photon Emission Computed Tomography (SPECT) is a standard imaging modality in nuclear medicine, especially in the cardiology segment. SPECT images provide the basis for clinical diagnosis of coronary artery disease, and combined with an attenuation map provided e.g. by computed tomography, the evaluation of absolute tracer uptake will be possible. Necessary pre-conditions for quantitative imaging are a model of sensitivity and spatial resolution of SPECT detectors and the understanding of reconstruction properties [1]. In this paper we present an assessment of reconstruction image quality based on an analysis of filtered back-projection, an analytic reconstruction method that is still standard for computed tomography [2]. For SPECT imaging, iterative methods like MLEM [3] and OSEM [4] are preferred for their noise performance and the possibility to correct for attenuation, spatial resolution, scatter, and cross-contamination of different radioisotopes [5]. We investigate FBP and OSEM using software phantoms and evaluate the performance of these reconstruction methods in terms of signal and power spectra, a method known as the Detective Quantum Efficiency (DQE) model from x-ray imaging.

2   Materials and Methods

Description of image quality is based on a contrast phantom, a cylinder of radius r_b with a spherical lesion of radius r_l in its centre. Activity is measured by a

SPECT detector with parallel hole collimator, characterized by square detector pixels of pitch p and detector efficiency E, defined by NEMA system planar sensitivity [6].

The SPECT image is reconstructed from projections taken under different viewing angles equally spread over $360°$ during the imaging time T.

Activity per voxel is given in units of Becquerel, specified as A_l and A_b in the lesion and background region, respectively. When we take a transaxial slice of thickness p and measure the radiation from the phantom slice with a detector in close contact, the average number of background counts per pixel in the detector is $n_b = A_b TE$, and the signal-to-noise ratio is $SNR_0 = \sqrt{A_b TE}$.

Lesion detectability is described by the Rose criterion, stating that the contrast-to-noise ratio $CNR = \Delta S/N$ has to be larger than a value $k \approx 5$ [7]. With the lesion contrast C_0 we get $CNR_0 = C_0 \cdot SNR_0 \cdot \sqrt{r_l^2 \pi/p^2}$. We use a software phantom with $r_b = 75$mm, $r_l = 25$mm, voxel size $p = 3$mm extend our theory to statistical reconstruction. To speed up simulation we calculate the central transaxial slice of the phantom in 2D cylinder geometry. With a background activity of 70MBq per litre, a square hole collimator with $E = 1.99 \cdot 10^{-4}$ ($L = 30$mm septa length, $D = 1.5$mm hole size, infinite septa absorption at negligible septa thickness), 128 projection angles and 20s time per view we calculate a reconstructed signal value of $A_b TE = 995$ counts per voxel.

Detector resolution is considered analytically in our simulation. When the collimator is 5mm away from the phantom surface, spatial resolution in the phantom centre is calculated as $R = 5.5$ mm parallel to the detector axes, equivalent to a Gaussian distribution with $\sigma = R/2p\sqrt{2\ln 2} = 0.78$ voxels.

Noise Power Spectra are extracted by Fourier analysis of the centre part of the reconstructed phantom without lesion. We use a 16×16 pixel region, apply a one-dimensional Fourier transform on 16 rows with their respective mean values subtracted, and take the average of the squared moduli to generate the noise power spectra. All spectra are symmetrically defined in the frequency range $-0.5\ldots0.5$ in units of cycles per pixel. By definition, the integral of the NPS function is equal to the background variance of the image.

Signal Power Spectra are derived by Fourier transformation of a differentiated step function. We differentiate the edge of the lesion with contrast $C_0 = 1$ in a noise free image along one of the detector axes, apply a one-dimensional Fourier transform on 16 data values centred on the lesion edge, and calculate the signal power spectra from the squared moduli. The zero frequency value of the SPS function is equal to the step height at the lesion edge which is, for ideal SPECT, given by $SPS(0) = C_0 \cdot A_b TE$. The normalized SPS function is better known as the squared modulation transfer function, MTF^2.

3   Results

In the following we start with the evaluation of FBP and OSEM for ideal projections, and then add corrections for attenuation and detector resolution in statistical reconstruction.

3.1   Ideal SPECT

In filtered back-projection the signal of all detector pixels is added up and spatially filtered so that the value for the number of counts in a central voxel is restored [2]. Noise is added on all voxels along the lines of back-projection, resulting in an inverse square root dependence on the number of pixels per phantom diameter, $SNR = SNR_0 \sqrt{p/2r_b Q}$, with Q describing the effect of the filter function [1]. The same holds for the contrast-to-noise ratio CNR_0. Simulated data show perfect agreement with this noise theory.

Fig. 1 shows noise power spectra for ideal SPECT reconstructed with FBP and linear interpolation to avoid streaking, in comparison to OSEM reconstruction, both shown smoothed with B-splines. For Ram-Lak and Shepp-Logan filters we find a nearly white spectrum at lower frequency and moderate noise reduction at higher frequency due to linear interpolation. Cosine and Hann filters suppress noise strongly especially in the high frequency range, giving a different noise texture. Additionally, noise is reduced throughout the whole frequency range.

Iterative reconstruction is known for soft, low-noise images at low iteration numbers and for sharper images and higher noise at a high number of iterations. For OSEM with low iteration numbers we see that noise power spectra decrease exponentially by nearly one order of magnitude from zero to 0.5 cycles per pixel. Duplication of the iteration numbers shifts up the noise power spectra by a factor of two or three, with a slight saturation in the lower frequency part. After 16 iterations the noise spectrum is approximately white, with somewhat lower values in the low and high frequency range.

Signal power spectra for ideal SPECT show the limited recovery of the high frequency signal due to linear interpolation and different filters, most prominent for the Hann filter (Fig. 2). Taking the measured curve for Ram-Lak as a reference for the impact of linear interpolation and multiplying by the squared theoretical filter functions we get the SPS curves for FBP with linear interpolation. The resulting data points (open symbols) show an excellent agreement with the measured signal power spectra.

With OSEM, after one iteration only the lowest frequency part of the spectrum is entirely recovered while the high frequency part is completely lost. With each doubling of iteration numbers the spectra are shifted up roughly by a factor of three before they saturate at the theoretically achievable signal level. With too high iteration numbers artifacts and artificial structures appear in the SPS.

3.2   Phantom Size Dependence

Fig. 3 shows SPS and NPS for two phantoms of different size in comparison. For the larger phantom, exactly the doubled number of iterations is needed to get the same SPS spectra as for the standard phantom, and the resulting noise power spectra are two times higher than for the smaller phantom. This is exactly the same phantom size dependence as for filtered back-projection.

3.3   Spatial Resolution

Correction for detector resolution is implemented in iterative reconstruction by application of a Gaussian filter in forward projection. We have to apply slightly smaller σ values than calculated to avoid overshoots in the power spectra. Fig. 4
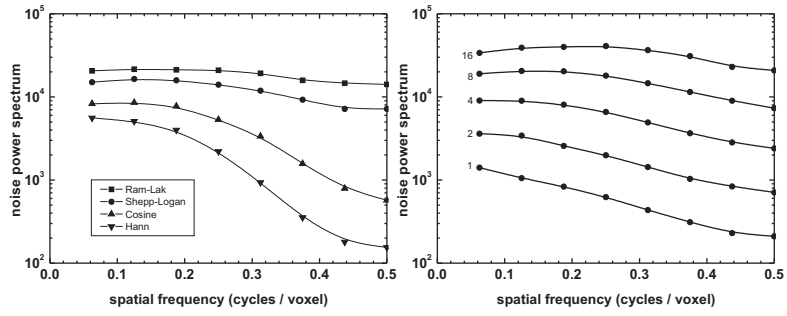

Fig. 1.   Noise power spectra for ideal SPECT, FBP with linear interpolation and different filters (left), and OSEM, subset size 16, with number of iterations (right).
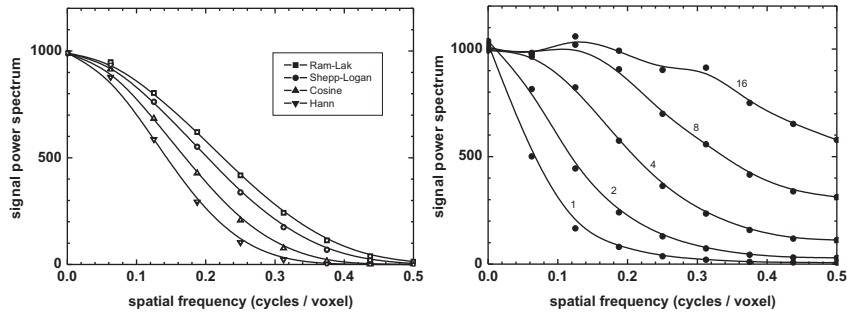

Fig. 2. Signal power spectra for FBP (left) and OSEM (right) as in Fig. 1.
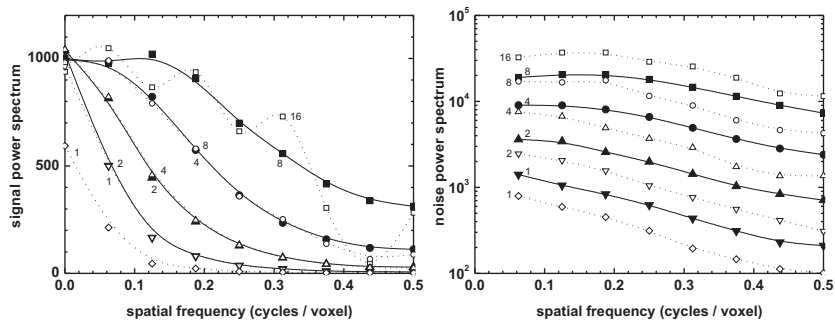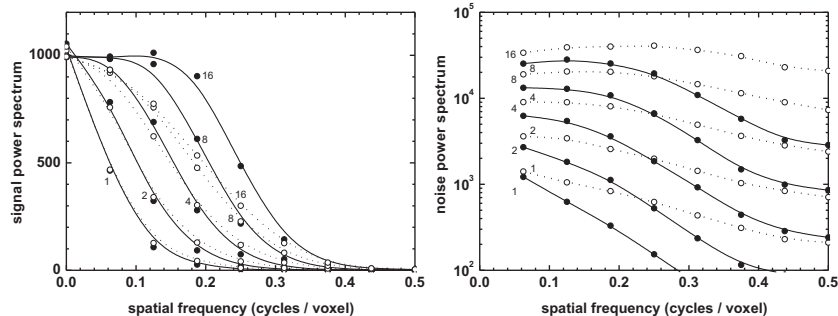

Fig. 3. Signal and noise power spectra for OSEM, subset size 16. Standard phantom (solid lines, full symbols) and 2 x larger phantom (dotted lines, open symbols).

Fig. 4. Signal (left) and noise power spectra (right) for OSEM with resolution recovery (solid lines) in comparison to uncorrected data (dotted lines).

shows the improved SPS for resolution correction with $\sigma = 0.65$ (solid lines) in comparison to uncorrected data (dotted lines). With a sufficient number of iterations we see that higher frequency signals can be recovered. The method is however limited by reconstruction time and increased noise. In the corresponding noise power spectra we see a general noise reduction, compared to uncorrected data, caused by resolution recovery, especially in the high frequency range. The variance of the image in this example is reduced by a factor of two.

4   Discussion

We present a theory describing the impact of reconstruction on image quality, providing quantitative measures for the assessment of reconstruction methods. We find a comparable behaviour of FBP and OSEM with reference to the object size. Directions are given how to optimize image quality in nuclear medicine by OSEM with the right choice of iteration numbers and use of resolution recovery. Future work will determine the limits of absolute quantification of tracer uptake.

References

1. Wieczorek H, Goedicke A. Analytical model for spect detector concepts. IEEE Trans Nucl Sci. 2006;53(3):1102–12.
2. Kak A, Slaney M. Principles of Computerized Tomographic Imaging. New York, IEEE Press; 1987.
3. Shepp L, Vardi Y. Maximum likelihood reconstruction for emission tomography. IEEE Trans Med Imaging. 1982;1(2):113–22.
4. Hudson, H M , Larkin, R S. Accelerated image reconstruction using ordered subsets of projection data. IEEE Trans Med Imaging. 1994;13(4):601–9.
5. Dey, T , Wieczorek, H , Backus, B , et al. Thallium-Stress, Technetium-Rest Protokoll für Cardiac SPECT. Proc BVM. 2010;in press.
6. NEMA standards publication NU1-2001. Rosslyn, VA USA, National Electrical Manufacturers Association; 2001.
7. Rose A. Advances in Electronics. Academic, New York; 1948.